JOURNAL OF VIROLOGY, Dec. 2006, p. 12283–12292 Vol. 80, No. 24
0022-538X/06/$08.00+0 doi:10.1128/JVI.00889-06

Indolopyridones Inhibit Human Immunodeficiency Virus Reverse Transcriptase with a Novel Mechanism of Action▽

Dirk Jochmans,[1]* Jérôme Deval,[2] Bart Kesteleyn,[1] Herwig Van Marck,[1] Eva Bettens,[1] Inky De Baere,[1] Pascale Dehertogh,[1] Tania Ivens,[1] Marcia Van Ginderen,[1] Bertrand Van Schoubroeck,[1] Maryam Ehteshami,[2] Piet Wigerinck,[1] Matthias Götte,[2] and Kurt Hertogs[1]

Tibotec BVBA, Generaal De Wittelaan L 11B 3, 2800 Mechelen, Belgium,[1] and Department of Microbiology and Immunology, McGill University, Duff Medical Building (D-6), 3755 University Street, Montreal, Quebec H3A 2B4, Canada[2]

Received 2 May 2006/Accepted 26 September 2006

We have discovered a novel class of human immunodeficiency virus (HIV) reverse transcriptase (RT) inhibitors that block the polymerization reaction in a mode distinct from those of the nucleoside or nucleotide RT inhibitors (NRTIs) and nonnucleoside RT inhibitors (NNRTIs). For this class of indolopyridone compounds, steady-state kinetics revealed competitive inhibition with respect to the nucleotide substrate. Despite substantial structural differences with classical chain terminators or natural nucleotides, these data suggest that the nucleotide binding site of HIV RT may accommodate this novel class of RT inhibitors. To test this hypothesis, we have studied the mechanism of action of the prototype compound indolopyridone-1 (INDOPY-1) using a variety of complementary biochemical tools. Time course experiments with heteropolymeric templates showed "hot spots" for inhibition following the incorporation of pyrimidines (T>C). Moreover, binding studies and site-specific footprinting experiments revealed that INDOPY-1 traps the complex in the posttranslocational state, preventing binding and incorporation of the next complementary nucleotide. The novel mode of action translates into a unique resistance profile. While INDOPY-1 susceptibility is unaffected by mutations associated with NNRTI or multidrug NRTI resistance, mutations M184V and Y115F are associated with decreased susceptibility, and mutation K65R confers hypersusceptibility to INDOPY-1. This resistance profile provides additional evidence for active site binding. In conclusion, this class of indolopyridones can occupy the nucleotide binding site of HIV RT by forming a stable ternary complex whose stability is mainly dependent on the nature of the primer 3′ end.

The reverse transcriptase (RT) enzyme of human immunodeficiency virus type 1 (HIV-1) remains a major target in antiretroviral therapy, with the current standard of care being the use of two nucleoside or nucleotide analogue reverse transcriptase inhibitors (NRTIs), combined with one nonnucleoside reverse transcriptase inhibitor (NNRTI) or protease inhibitor (32).

Upon entry into the cell, the virus is uncoated, and the viral RT enzyme converts its single-stranded RNA genome into double-stranded proviral DNA. Inhibition of this crucial event in the early viral life cycle ultimately precludes the virus from proliferating. Following the intracellular phosphorylation of NRTIs, NRTI-triphosphates compete with natural deoxyribonucleoside triphosphate (dNTP) pools and bind to the RT active site. They act as chain terminators due to the lack of a 3′-hydroxyl group (31). In contrast, NNRTIs represent a chemically diverse class of compounds that bind to a pocket in the vicinity of the catalytic site (25, 29, 30). Binding of these inhibitors is noncompetitive with respect to both dNTPs and template/primer (16).

Despite the potency of combinations of NRTIs and NNRTIs, the emergence of mutations conferring resistance remains a major cause for treatment failure. The advent of novel RT inhibitors with a different mechanism of action and their use in combination with NRTIs and/or NNRTIs may provide a strategy to compromise the activity of the enzyme to an extent that further reduces the risk of developing resistance.

We discovered a series of RT inhibitors that behave neither like NRTIs nor like NNRTIs. Although structurally unrelated to nucleotides, we provide strong evidence that members of this family of compounds can occupy the active site of the enzyme and compete with natural dNTP substrates.

MATERIALS AND METHODS

Reagents. All reagents used for chemical synthesis, enzymatic reactions, and cell culture were purchased from commercial sources and used as such.

Marketed anti-HIV compounds. The NNRTIs efavirenz (Sustiva; Bristol-Myers Squibb) and nevirapine (Viramune; Boehringer Ingelheim) and the NRTIs abacavir (Ziagen; GlaxoSmithKline), didanosine (Videx; Bristol-Myers Squibb), emtricitabine (Emtriva; Gilead), lamivudine (Epivir; GlaxoSmithKline), stavudine (Zerit; Bristol-Myers Squibb), tenofovir (Viread; Gilead), zalcitabine (Hivid; Roche), and zidovudine (Retrovir; GlaxoSmithKline) were purified from the commercial formulations.

Chemical synthesis of INDOPY-1. Indolopyridone-1 (INDOPY-1) was synthesized essentially as described elsewhere (15). Briefly, synthesis started with the condensation of commercially available *N*-acetyl-3-hydroxyindole with 4-nitroaniline, under refluxing conditions in acetic acid, yielding 1-[3-(4-nitro-phenylamino)-indol-1-yl]-ethanone. After deacylation with triethylamine in refluxing methanol, the intermediate was further formylated using phosphorus oxychloride in dimethylformamide to yield 3-(4-nitro-phenylamino)-1*H*-indole-2-carboxaldehyde (27). Knoevenagel condensation of this intermediate with ethyl cyanoacetate in the presence of a catalytic amount of triethylamine gave 2-cyano-3-[3-(4-nitro-phenylamino)-1*H*-indol-2-yl]-2-propenoic acid ethyl ester whose intramolecular cyclization under reflux in 1,2-ethanediol yielded 1-(4-nitro-phenyl)-2-oxo-2,5-dihydro-1*H*-pyrido[3,2-b]indole-3-carbonitrile (26). In a last step, N methylation using methyl iodide led to INDOPY-1.

* Corresponding author. Mailing address: Tibotec BVBA, Generaal De Wittelaan L 11B 3, 2800 Mechelen, Belgium. Phone: 32 15 401 208. Fax: 32 15 444 374. E-mail: djochman@tibbe.jnj.com.

▽ Published ahead of print on 4 October 2006.

Cells and viruses. The human T lymphotropic virus type 1-transformed human T lymphoblastoid cell line MT4 was kindly provided by Naoki Yamamoto (National Institute of Infectious Diseases, AIDS Research Center, Tokyo, Japan). Human lymphocyte CEM cells were obtained from the American Tissue Cell Culture Collection (Manassas, Virginia). Both cell lines were maintained in RPMI 1640 medium supplemented with 10% heat-inactivated fetal calf serum, 2 mM L-glutamine, 0.1% $NaHCO_3$, and antibiotics (0.02% gentamicin, 0.8% G418) and incubated in a humidified incubator with a 5% CO_2 atmosphere at 37°C. Peripheral blood mononuclear cells (PBMC) were purified from HIV-negative donors and activated as previously described (7). MT4-LTR-EGFP cells were obtained by transfecting MT4 cells with a selectable construct encompassing the sequences coding for the HIV long terminal repeat (LTR) as a promoter for the expression of enhanced green fluorescent protein (EGFP) and subsequent selection of permanently transfected cells.

HIV-1 IIIB and HIV-2 ROD were provided by Guido van der Groen (Institute of Tropical Medicine, Antwerp, Belgium). Simian immunodeficiency virus (SIV) Mac251 was obtained from Martin Cranage (Department of Cellular and Molecular Medicine, St. George's Hospital Medical School, London, United Kingdom) and Ronald Desrosiers (New England Primate Research Center, Harvard Medical School, Southborough, Massachusetts).

Recombinant HIV-1 viruses, derived from clinical samples, were constructed as previously described by cotransfection of MT4 cells with sample-derived viral protease- and RT-coding sequences and an HIV-1 HXB2-derived proviral clone deleted in the protease- and RT-coding region (10).

Site-directed mutant RT-coding sequences were generated from a pGEM vector containing the HIV-1 clone HXB2 protease- and RT-coding sequence by using a QuikChange site-directed mutagenesis kit (Stratagene) and high-performance liquid chromatography-purified primers (Genset Oligos). Plasmids were sequenced to confirm that they contained the desired mutations. Mutant viruses were created by recombination of the mutant protease-RT sequence with a protease-RT-deleted HIV-1 HXB2 proviral clone (10).

Antiviral assays. The antiviral activity on different HIV-1 strains, HIV-2 ROD and SIV Mac251, was determined in a cell-based virus replication assay. Here MT4-LTR-EGFP cells (150,000 cells/ml) are infected (multiplicity of infection [MOI] of 0.01) in the presence or absence of different inhibitor concentrations. After 3 days of incubation, the amount of virus replication is quantified by measuring the EGFP fluorescence and expressed as the 50% effective concentration (EC_{50}). The toxicity of inhibitors is determined in parallel on mock-infected MT4 cells (150,000 cells/ml) stably transformed with a CMV-EGFP reporter gene and cultured in the presence or absence of test compound concentrations. After 3 days of incubation, cell proliferation is quantified by measuring the EGFP fluorescence and expressed as CC_{50} values (cytotoxic concentration of drug which reduced the viable cell number by 50%).

Determination of anti-HIV-1 activity and toxicity in CEM cells was done by an 3-(4,5-dimethylthiazol-2-yl)-2,5-diphenyltetrazolium bromide (MTT)-based colorimetric cytopathic effect protection assay (24).

Anti-HIV-1 activity and toxicity in a PBMC-based antiviral assay with a p24-based readout was measured as previously described (7).

The procedure to determine the activity against C-type retrovirus murine Moloney sarcoma virus (Mo-MSV) was performed as described previously (2). Briefly, murine fibroblast (C3H) cells were seeded into wells (diameter of 2.3 cm) of tissue culture plates at 5×10^4 cells per ml. The cell cultures were infected 24 h later with 150 focus-forming units of MSV for 90 min at 37°C, and then the medium was replaced with 1 ml of fresh culture medium containing various concentrations of the test compounds. After 6 days, the transformation of the cell cultures was examined microscopically.

INDOPY-1 activities against Mo-MSV, coxsackievirus, parainfluenza virus, poliovirus, reovirus, rhinovirus, Semliki Forest virus, Sindbis virus, vesicular stomatitis virus, human cytomegalovirus, herpes simplex virus (type I or II), vaccinia virus, and varicella-zoster virus were determined at the Rega Institute (Leuven, Belgium).

Time of drug addition assay. For the time of addition assay, MT4-LTR-EGFP cells were infected with HIV-1 IIIB at a high MOI of 0.2 and centrifuged for 10 min at 1,200 × *g*. Two washing steps were carried out at 4°C to remove nonadsorbed virus and to synchronize the infection before the cells were transferred to a 37°C incubator. From 30 min postinfection onwards, the compounds to be tested were added to parallel cultures at different time points. Final compound concentrations were at least 10 times in excess of their EC_{50}. At 24 h postinfection, the cultures were scored microscopically for fluorescence, and supernatants were tested for p24 concentration.

Reverse transcriptase assay. Reagents for the reverse transcriptase assay were purchased from Amersham (TRK1022 kit) and used according to the manufacturer's protocol with slight modifications. Standard RT inhibition assays were performed in 50-μl volumes containing 0.5 μM [^{3}H]dTTP, 10 mg/ml poly(rA) · poly(dT)-coated scintillation proximity assay imaging beads, 50 mM Tris-HCl (pH 8), 80 mM KCl, 10 mM $MgCl_2$, 10 mM dithiothreitol, 2.5 mM EGTA, 0.05% (wt/vol) Nonidet P-40, 1% (vol/vol) dimethyl sulfoxide, and 2 nM recombinant HIV-1 reverse transcriptase (T3710Y). Reaction mixtures were incubated for 1 h at 37°C and stopped by adding 200 μl of 0.12 mM EDTA, pH 8.

Enzyme kinetics were performed as described previously (3). Reaction mixtures (50 μl) contained 50 mM Tris-HCl (pH 7.8), 5 mM dithiothreitol, 0.3 mM glutathione, 0.5 mM EDTA, 150 mM KCl, 5 mM $MgCl_2$, 1.25 mg/ml of bovine serum albumin, 0.015 mM poly(rA) · oligo(dT) template/primer, 0.06% Triton X-100, 2 nM HIV-1 RT, and different concentrations of [^{3}H]dTTP (3, 4, 6, 10, 20, and 40 μM; 2 μCi/assay) and INDOPY-1 (0, 0.25, 0.5, 1, and 2 μM). The reaction mixtures were incubated at 37°C for 30 min, at which time 200 μl of yeast RNA (2 mg/ml) and 1 ml of trichloroacetic acid (5% in 20 mM $Na_4P_2O_7$) were added. The solutions were kept on ice for 30 min, and then the acid-insoluble material was washed and analyzed for radioactivity. At least two measurements for each data point were performed. Data were fitted to the standard enzyme inhibition models (i.e., competitive, noncompetitive, and uncompetitive) using a nonlinear global curve-fitting program (GraphPad Prism version 4.0). Best fit was judged from the R^2 values.

Determination of RT inhibition in the presence of different templates/primers was performed using the procedure for enzyme kinetics. Apparent equilibrium dissociation constant ($K_{D(app)}$) values were estimated by fitting the data to the equation for single-site ligand binding using GraphPad Prism (version 4.0) as previously described (33).

Primer extension assay. DNA synthesis was performed with recombinant HIV-1 RT through use of a DNA/RNA primer/template hybrid (1). The primer/template hybrid (100 nM) was incubated together with wild-type HIV-1 RT (100 nM) in a buffer containing 50 mM Tris-HCl (pH 7.8), 60 mM NaCl, and 6 mM $MgCl_2$. dNTPs (10 μM) were added in the presence or absence of 6 μM INDOPY-1, and the reactions were allowed to proceed for 30 seconds or 1, 2, 5, 10, and 30 minutes. Control lanes included 3 μM ddCTP or dideoxythymidine triphosphate to assign the "hot spots" for INDOPY-1 inhibition.

Band shift experiments. The formation of ternary complexes was monitored with a radiolabeled primer (5′-TTAAAAGAAAAGGGGGGAC-3′). The labeled primer was preannealed to a threefold molar excess of the template (5′-CCTTCCAGTCCCCCCTTTTCTTTTAAAAAGT-3′). The DNA hybrid (50 nM) was then incubated with a 10-fold excess of wild-type HIV-1 RT enzyme. Increasing concentrations of INDOPY-1, dTTP, or nevirapine, ranging from 0 to 25 μM, were added to each sample and incubated for 15 min at room temperature. The complexes were subsequently challenged with 1.5 μg/μl heparin trap, followed by incubation for 1 h at room temperature. The samples were analyzed on 6% nondenaturing polyacrylamide gels.

Similar experimental conditions were applied when assessing the effects of variations at the 3′ end of the primer on the stability of the complex with INDOPY-1. We utilized two different sets of sequences: 5′-TTAAAAGAAAAGGGGGGAN-3′ served as the primer strands, and the corresponding templates were 5′-CCTTCCANTCCCCCCTTTTCTTTTAAAAAGT-3′, whereby the underlined N represents one of the four bases. Primer and template were combined to allow formation of correct base pairs. The second set of sequences consisted of the following primers 5′-CTTTCAGGTCCCTGTTCGGGCGCCACTN and their complementary templates 5′-CGAACAAATCTCTACNAGTGGCGCCCGAACAGGGACCTGAAAGCGAA-3′.

Competition between INDOPY-1 and the nucleotide substrate. The primer 5′-TTAAAAGAAAAGGGGGGA-3′ was annealed to a twofold molar excess of template 5′-CCTTCCAGTCCCCCCTTTTCTTTTAAAAAGT-3′. The DNA/DNA substrate was then incubated at 37°C with 2.5-fold excess of RT enzyme along with 10 μM ddCTP and 6 mM $MgCl_2$ for 30 min. The chain-terminated DNA/DNA-RT complex was incubated at room temperature with 3.1 nM radiolabeled dTTP to obtain a maximum in complex formation. Increasing concentrations of INDOPY-1 (0 to 12.5 μM) were added and allowed to incubate for 10 min. Samples were then analyzed on 6% nondenaturing polyacrylamide gels.

Site-specific footprinting. Site-specific footprints with Fe^{2+} were monitored on 3′-end-labeled DNA templates, as recently described (20). Briefly, hybridization of the template (150 nM) with the complementary primer (600 nM) was conducted in a buffer containing 20 mM sodium cacodylate (pH 7), and 20 mM NaCl. The duplex was incubated with HIV-1 RT (900 nM) in a buffer containing 120 mM sodium cacodylate (pH 7), 20 mM NaCl, 6 mM $MgCl_2$, and a mixture of nucleotide triphosphates that allow quantitative chain termination. Prior to the treatment with Fe^{2+}, complexes were preincubated at 37°C for 10 min with increasing concentrations of INDOPY-1, nevirapine, or dGTP. Treatment with Fe^{2+} was performed essentially as described before (20).

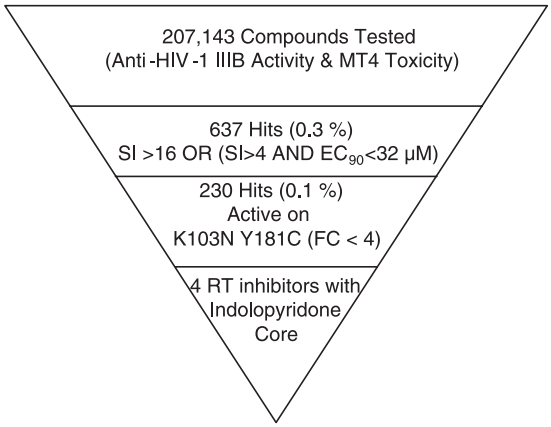

FIG. 1. Identification of INDOPY-1 from a high-throughput screening campaign. The triangle shows the screening cascade that resulted in the identification of a cluster of four active indolopyridones from a library of over 200,000 commercially available synthetic compounds with drug-like properties (Lipinsky rule of 5). Starting from an anti-HIV activity and a toxicity assay, in which molecules were tested at up to 32 μM, over 600 selective HIV inhibitors where identified using the indicated criteria (SI, selectivity index). The majority showed a loss of activity on the NNRTI-resistant strain (K103N Y181C), and these compounds were therefore not further pursued. From the remaining 230, four were found to be RT inhibitors in an enzymatic assay. This set of compounds, which included INDOPY-1, had a very similar chemical scaffold, the indolopyridone core.

Genotyping and subtype determination. Genotypic analysis was performed by automated population-based full-sequence analysis (ABI PRISM BigDye Terminator cycle sequencing). Sequencing results are reported as amino acid changes compared to the HIV-1 wild-type (HXB2) reference sequence (19). Subtypes were determined by heteroduplex mobility assay (6) or sequencing.

In vitro selection experiments. MT4-LTR-EGFP cells were infected with HIV-1 wild-type strain IIIB at an MOI of 0.01 to 0.001 times the 50% cell culture infectious dose per cell in the presence of INDOPY-1 at three times the EC_{50}. This corresponded to an initial infection rate of ~1%. Cultures were subcultivated in the presence of the same concentration of inhibitor every 3 to 4 days and microscopically examined for signs of virus replication. At 100% virus breakthrough, the supernatant was collected and stored as a new virus strain. These new virus strains were used to infect fresh cultures in the presence of a higher concentration of INDOPY-1. The procedure was repeated up to a concentration of 2.4 μM. Viral breakthrough was assessed by microscopic scoring of the cytopathogenicity and virus-induced fluorescence. A viral breakthrough of 100% was defined as microscopic evidence of extensive viral replication in all cell clusters (full cytopathic effect). Samples for genotyping were obtained from the harvested supernatant.

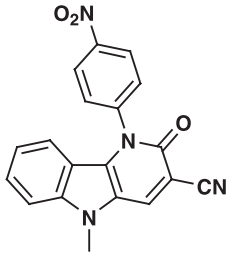

FIG. 2. Chemical structure of INDOPY-1. 5-Methyl-1-(4-nitrophenyl)-2-oxo-2,5-dihydro-1H-pyrido[3,2-b]indole-3-carbonitrile.

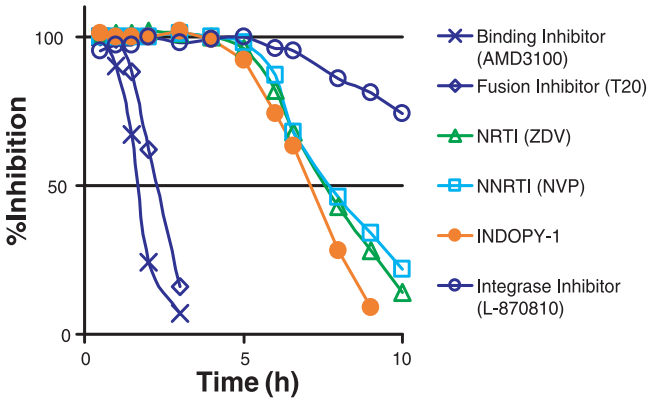

FIG. 3. Time of drug addition. Parallel cultures of MT4-LTR-EGFP cells with synchronized HIV-1 IIIB infection were treated with HIV inhibitors at the indicated time points. Final compound concentrations were at least 10-fold higher than the EC_{50}s: 1 μM AMD3100, 1 μM T20, 10 μM zidovudine (ZDV), 1 μM nevirapine (NVP), 10 μM INDOPY-1, and 10 μM L-870810.

RESULTS AND DISCUSSION

Discovery of a novel class of competitive RT inhibitors. INDOPY-1 was identified during a high-throughput screening campaign that evaluated more than 200,000 compounds for anti-HIV activity (Fig. 1). Compounds were profiled for inhibition of wild-type HIV-1 IIIB replication (EC_{50}) and cytotoxicity (CC_{50}) in a sensitive MT4 cell system, using a HIV-responsive reporter gene readout (24). Since the objective of this screening campaign was to focus on anti-HIV molecules with a novel mechanism of action, we further assayed promising hits with an HIV-1 strain that carried NNRTI resistance-associated mutations K103N and Y181C (4).

Four selective HIV-1 inhibitors that remained active against this NNRTI-resistant strain have a very similar indolopyridone core. In our MT4 cell system, the most potent compound within this series, herein referred to as INDOPY-1 (Fig. 2), showed an EC_{50} for the wild-type HIV-1 IIIB strain of 30 nM. The selectivity index (CC_{50}/EC_{50}) associated with INDOPY-1 was over 300 in this system. In human T lymphotropic virus type 1-free CEM cells the EC_{50} was 25 nM with a corresponding selectivity index of over 2,000. In fresh PBMC cultures, INDOPY-1 inhibited HIV replication by 50% at 100 nM, with a selectivity index of over 1,000.

We conducted a time of drug addition assay to identify the viral target (Fig. 3). Test compounds were added at several time points to a cell-based system with synchronized HIV-1

TABLE 1. Inhibition of DNA synthesis with different template/primers

Drug	IC_{50} (μM)[a]			
	Poly(rA) · poly(dT)	Poly(rI) · poly(dC)	Poly(rC) · poly(dG)	Poly(rU) · poly(dA)
INDOPY-1	0.29 ± 0.07	1.10 ± 0.15	>200	>100
Zidovudine-TP	0.011 ± 0.010	>100	>100	>100
Efavirenz	0.24 ± 0.08	0.22 ± 0.06	0.022 ± 0.012	0.11 ± 0.11

[a] IC_{50}, 50% inhibitory concentration. Average and standard deviation of at least three independent measurements.

TABLE 2. Antiviral activity of INDOPY-1 on different retroviruses

Virus	EC_{50} (μM) ± SD[a]
HIV-1 IIIB	0.03 ± 0.01
HIV-1 HXB2 K103N Y181C	0.10 ± 0.06
HIV-2 ROD	0.18 ± 0.03
SIV Mac251	0.21 ± 0.08
Mo-MSV	>10

[a] Average and standard deviation of at least three independent measurements.

infection (23). We observed that INDOPY-1, like NRTIs and NNRTIs, potently inhibited HIV-1 replication when added within 7 h postinfection. In contrast, inhibitors targeting the entry and/or fusion process blocked viral replication only when added within 1 hour postinfection. Integrase inhibitors showed antiviral effects when added 8 hours postinfection. These data provided the first evidence that INDOPY-1 interferes with the reverse transcription step of HIV. This was confirmed in a cell-free assay using purified wild-type HIV-1 RT and a homopolymeric poly(rA) · poly(dT) template/primer (23). INDOPY-1 inhibited the incorporation of [^{3}H]dTTP with a 50% inhibitory concentration of 290 nM (Table 1).

We tested a broad panel of RNA as well as DNA viruses to further assess the specificity of the antiviral activity of INDOPY-1 (Table 2). In contrast to NNRTIs (34), INDOPY-1 remained active against the HIV-1 K103N Y181C mutant strain (EC_{50} = 100 nM), the HIV-2 strain ROD (EC_{50} = 180 nM), and against the SIV strain Mac251. These characteristics are reminiscent of NRTIs and differ significantly from NNRTIs that do show reduced susceptibility (>100-fold) on all of the aforementioned strains (5). However, the C-type retrovirus Mo-MSV as well as various RNA viruses (coxsackievirus, parainfluenza virus, poliovirus, rhinovirus, Semliki Forest virus, Sindbis virus, vesicular stomatitis virus, and reovirus) and DNA viruses (herpes simplex virus [type I or II], vaccinia virus, varicella-zoster virus, and human cytomegalovirus) were all insensitive to INDOPY-1 (EC_{50} > 10 μM). So far, no virus outside the family of *Lentiviridae* was found to be sensitive to the inhibitory activity of INDOPY-1, specifically distinguishing INDOPY-1 from the NRTIs that inhibit a broader spectrum of viral polymerases (5).

Mode of inhibition of DNA synthesis by INDOPY-1. Given that INDOPY-1 remains active against HIV-2 and NNRTI-resistant strains, it is likely that the mechanism of action associated with INDOPY-1 differs from that of NNRTIs. Moreover, the lack of both a ribose sugar and a nucleobase moiety points to mechanistic differences between INDOPY-1 and NRTIs. To further test this hypothesis, we investigated whether INDOPY-1 acts as a competitive, noncompetitive, or uncompetitive inhibitor with respect to the dNTP substrate. Steady-state kinetics with saturating concentrations of homopolymeric poly(rA) · poly(dT) template/primers and various concentrations of [^{3}H]dTTP substrate and INDOPY-1 was performed. Fitting the data to the competitive, noncompetitive, and uncompetitive models of enzyme inhibition showed R^2 values of 0.98, 0.89, and 0.81, respectively, indicating that inhibition by INDOPY-1 is best described as competitive (Fig. 4). The analysis yielded a K_m (dTTP) of 2.1 ± 0.26 μM and a K_i of 0.16 ± 0.02 μM. These findings show that INDOPY-1 competes with the incoming dNTP for binding RT. NRTIs are also competitive RT inhibitors (8, 9); however, they require intracellular phosphorylation for activity (8). In contrast, INDOPY-1 does not require metabolic activation. The competitive mode of inhibition strongly suggests that the binding site of INDOPY-1 overlaps with the nucleotide binding site (N-site) of RT.

INDOPY-1 reversibly binds the RT active site independent of base-like complementarities with the template. Then we tested the inhibitory effects of INDOPY-1 with alternative nucleic acid substrates to analyze whether the homopolymeric poly(rA) · poly(dT) template/primer may provide a unique structural environment that facilitates INDOPY-1 binding (Table 1). It was found that inhibition of DNA synthesis was

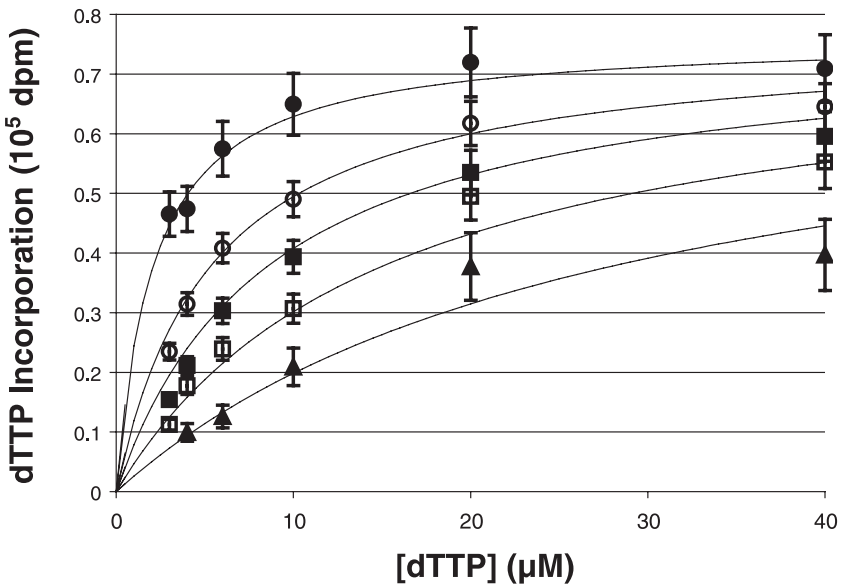

FIG. 4. Fitted curves for the competitive model for INDOPY-1 inhibition of HIV-1 RT. HIV-1 RT was incubated for 30 min at 37°C with various concentrations of INDOPY-1 (●, 0 μM; ○, 0.25 μM; ■, 0.5 μM; □, 1 μM; ▲, 2 μM) and dTTP concentrations as indicated.

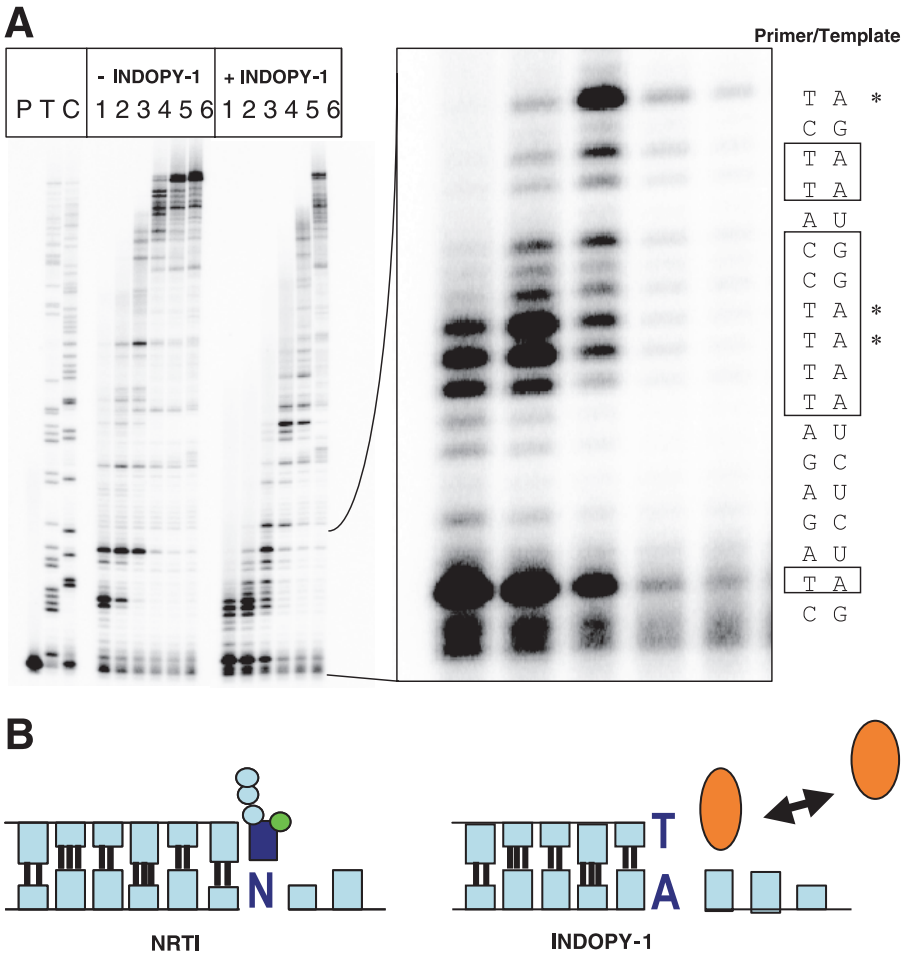

FIG. 5. Sequence dependence of INDOPY-1-mediated inhibition of DNA synthesis. (A) Inhibition of DNA synthesis was monitored in time course experiments in the absence (−) and presence (+) of INDOPY-1, using a heteropolymeric DNA/RNA primer/template substrate. The sequence ahead of the primer 3′ end is shown on the right. Lane P, control in the absence of Mg^{2+}; lanes T and C, reaction mixtures in the presence of dideoxythymidine triphosphate and ddCTP, respectively. Lanes 1 to 6 show different reaction times: 30 s and 1, 2, 5, 10, and 30 min, respectively. (B) Sequence parameters that affect inhibition by NRTIs and INDOPY-1. Primer/template sequences are shown as light blue rectangles. Binding of NRTIs or the next nucleotide (blue rectangle) is determined by the nature of the base of the template (N) ahead of the primer. Inhibition by INDOPY-1 (orange oval) follows predominantly the incorporation of a thymidine.

less pronounced with poly(rI) · poly(dC), while no inhibition was detected using poly(rC) · poly(dG) or poly(rU) · poly(dA) template/primer. This is different from NNRTIs (efavirenz) that show increased inhibitory activity with poly(rC) · poly(dG) and from zidovudine-TP that is inhibitory only when a poly(rA) · poly(dT) template/primer is used. To reconcile these data, we studied inhibition of DNA synthesis through the use of heteropolymeric RNA/DNA substrates (Fig. 5) (20). The time course in the absence of INDOPY-1 shows the formation of a final product that corresponds to the length of the tem-

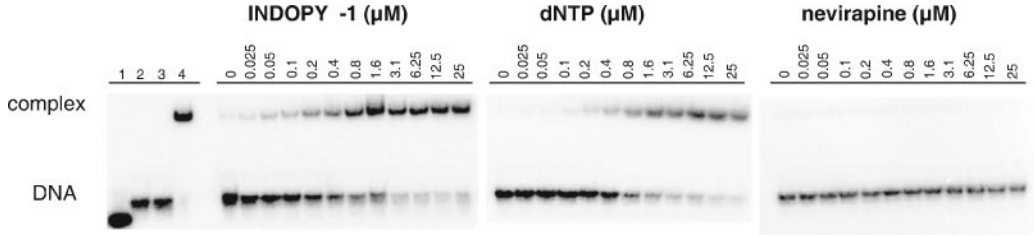

FIG. 6. Stabilization of preformed RT-DNA/DNA complexes with INDOPY-1. Preformed RT-DNA/DNA complexes were incubated with increasing concentrations of INDOPY-1 (left), the next complementary nucleotide (middle), or nevirapine (right). These complexes were challenged with heparin to trap dissociated RT molecules before the samples were analyzed on a nondenaturing gel. Lane 1 shows the labeled primer, and lanes 2, 3, and 4 are controls in the absence of enzyme, preincubation with heparin, and in the absence of heparin, respectively.

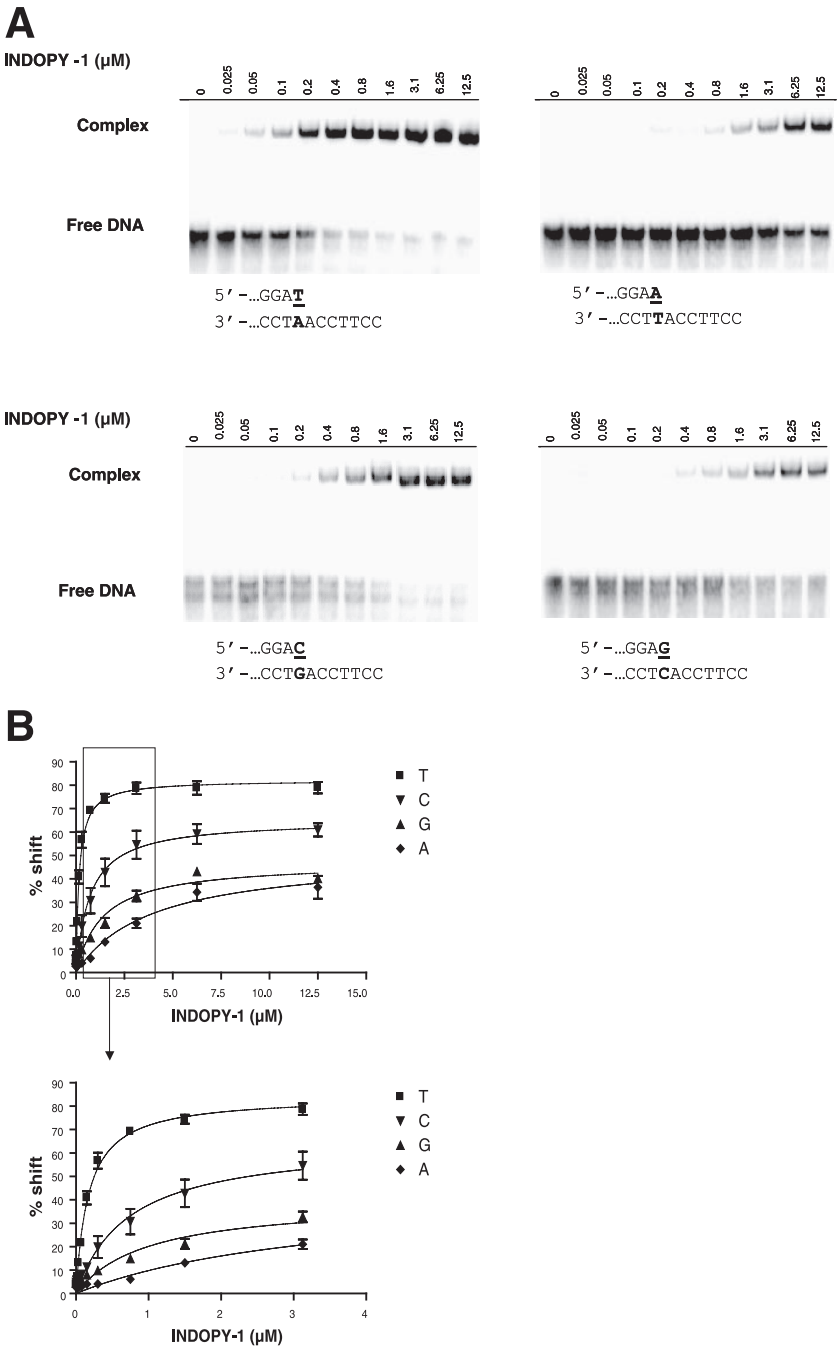

FIG. 7. Effect of the 3′ end of the primer on INDOPY-1 binding. (A) Preformed RT-DNA/DNA complexes containing variable residues at the 3′ end of the primer and the complementary template position were incubated with increasing concentrations of INDOPY-1. Complexes were challenged with heparin to trap dissociated RT molecules, and the samples were analyzed on a nondenaturing gel as shown in Fig. 6. The relevant sequences are shown below the band shift experiment. (B) Graphic representation of the data shown in panel A. T, thymidine; C, deoxycytidine; G, deoxyguanosine; A, deoxyadenosine. The lower concentration range of the graph on the top is also shown with an expanded *x* axis (below).

plate. Shorter reaction products point to enzyme pausing in the absence of INDOPY-1. In the presence of the inhibitor, additional, distinct bands appear following incorporation of pyrimidines (mainly thymidine). The next base in the template, ahead of the 3′ end of the primer, which determines the specificity of binding and incorporation of NRTIs through base pairing, does not appear to influence the inhibitory effects of INDOPY-1. Hot spots for INDOPY-1 inhibition are seen with all four bases at this template position (Fig. 5A). These bands disappear over time, which indicates that inhibitor binding is reversible and that the mechanism of action does not involve chain termination. These data show that binding of INDOPY-1 is not dependent on base-like complementarities with the template. Interactions with the enzyme appear to be favored

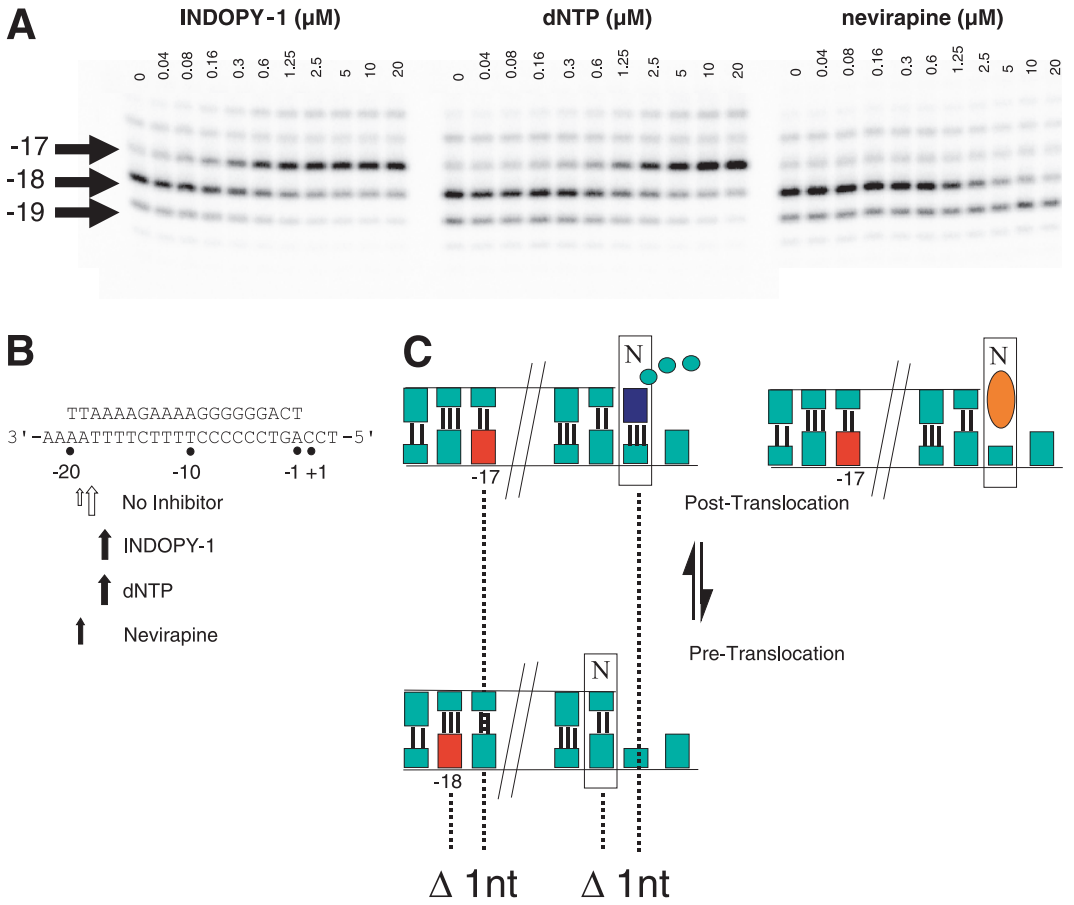

FIG. 8. Effect of INDOPY-1 on the translocational equilibrium of HIV-1 RT. (A) We employed a site-specific footprinting approach to determine the ratio of complexes that exist pre- or posttranslocation. The translocation state was monitored in the presence of increasing concentrations of INDOPY-1, the next nucleotide (middle), and nevirapine. (B) Schematic representation of results shown in panel A. Open arrows show cleavage positions in the absence of inhibitors. Filled arrows show cleavage positions at highest concentrations of inhibitors. The size indicates the relative cleavage intensity. (C) Model of INDOPY-1 binding. The position of the primer/template is shown relative to the nucleotide binding site. The lower complex represents the pretranslocational state, in which the N-site is occupied by the 3′ end of the primer terminus. The presence of the next nucleotide (blue rectangle) or the presence of INDOPY-1 (orange oval) can trap the complex in its posttranslocational state (top complex). nt, nucleotide.

with a pyrimidine at the primer terminus and/or with a purine in the template. This mode of recognition further distinguishes INDOPY-1 from NRTIs (Fig. 5B).

INDOPY-1 forms a stable ternary complex with HIV-1 RT. We studied whether a preformed RT-DNA/DNA complex can be stabilized with INDOPY-1, validating the RT nucleotide binding site as the target site for INDOPY-1 (Fig. 6). Previous band shift experiments have shown that increasing concentrations of the next complementary dNTP can stabilize a preformed RT-DNA/DNA complex (33). Here we show that INDOPY-1, similar to the templated nucleotide, can form a stable ternary complex. The presence of approximately 1,600 nM of the next dNTP (dTTP) shifted 50% of the labeled DNA substrate, and concentrations as low as 800 nM of INDOPY-1 are sufficient to cause the same effect. The presence of NNRTIs (nevirapine) does not stabilize this complex. For INDOPY-1, the stability of the ternary complex depends crucially on the nature of the 3′ end of the primer (Fig. 7), which is reflected in the estimation of the apparent K_D values. The K_D increases in the following order of the primer 3′-terminal nucleotide: thymidine ($K_{D(app)}$ = 0.16 ± 0.01 μM) < deoxycytidine ($K_{D(app)}$ = 0.72 ± 0.13 μM) < deoxyguanosine ($K_{D(app)}$ = 1.36 ± 0.25 μM) < deoxyadenosine ($K_{D(app)}$ = 3.9 ± 0.9 μM). When the experiment was performed with a different, unrelated sequence, the results showed the same trend: a thymidine and, to a lesser extent, a deoxycytidine at the 3′ end of the primer promotes binding of INDOPY-1. In this case, the stabilizing effect of INDOPY-1 is less pronounced, showing that inhibitor binding also depends on the sequence context (unpublished data). These findings provide direct evidence to show that INDOPY-1 binds preferentially following the incorporation of pyrimidines.

INDOPY-1 binds to the nucleotide binding site of RT after translocation and freezes the posttranslocation complex. Although the band shift experiments demonstrate the formation of a complex composed of RT, INDOPY-1, and the nucleic acid substrate, the data do not indicate whether INDOPY-1 and the nucleotide substrate bind to the same complex. Following catalysis, RT must translocate a single position further downstream to clear the nucleotide binding site. This config-

TABLE 3. Median change of INDOPY-1 susceptibility of HIV-1 strains derived from clinical isolates

Mutation pattern	Median fold change in EC_{50} compared to HIV-1 IIIB	Interquartile range (Q1–Q3)	No. of samples
Y115F M184V[a]	16	6.5–25	40
M184V[a]	3.6	2.0–5.8	566
K65R[a]	0.5	0.3–0.9	38
K65R M184V[a]	1.3	0.8–1.8	17
M41L L210W T215Y[b]	1.3	0.9–1.8	36
D67N K70R K219Q[b]	1.4	1.1–3.1	18
D67N K70R T215F K219Q[b]	1.2	0.9–2.8	12

[a] For each determination, viruses with additional mutations at positions 65, 115, or 184 were excluded.

[b] Viruses with mutations at positions 65, 115, or 184 were excluded from the analysis. Also for each determination, the viruses with additional mutations at positions 41, 67, 70, 210, 215, or 219 were excluded.

TABLE 4. Influence of different NRTI resistance-associated mutations on the susceptibility of INDOPY-1

HIV-1 HXB2 mutation(s) in RT	Fold change in $EC_{50} \pm SD$[a] compared to HIV-1 IIIB
TAMs (M41L D67N K70R T215Y)	3.0 ± 1.2
T69 insertion complex (T69S ins69-70S-S L210W T215Y)	0.9 ± 0.33
Q151M complex (A62V V75I F77L F116Y Q151M)	1.0 ± 0.27
Y115F M184V	>100
M184V	5.0 ± 2.6
Y115F	7.9 ± 1.6
K65R	0.5 ± 0.2
K65R M184V	0.9 ± 0.2

[a] Average and standard deviation of at least three independent measurements.

uration defines a posttranslocational state, in which the N-site of the enzyme can accommodate the next incoming dNTP, and the 3′ end of the primer occupies the priming site. In contrast, in the pretranslocational state, the N-site is still occupied by the previously incorporated dNTP, i.e., the novel 3′ end of the primer (28). Site-specific footprinting studies that allow tracking of the position of RT on its nucleic acid substrate at the resolution of a single nucleotide point to an equilibrium between both complexes (20). In these studies, the complex is incubated with Fe^{2+} ions that bind in close proximity to the RNase H active site of HIV-1 RT. Oxidation of the bound Fe ions produces a high local concentration of hydroxyl radicals that cleave the DNA template in a site-specific manner. We have chosen a sequence that exists mainly pretranslocation in the absence of nucleotides or inhibitors. Under these conditions, a major cut appears at position −18, and a minor cut appears at position −19 (Fig. 8A and B). The presence of the templated nucleotide (dTTP) causes a shift in the cleavage pattern. The major cleavage is now seen at position −17, which is indicative of the posttranslocation complex. An approximately 2 μM concentration of the templated nucleotide is required to trap 50% of the complex population in this posttranslocational state. INDOPY-1 is also able to freeze the posttranslocation complex, which provides strong evidence that INDOPY-1, like the natural nucleotide substrate, binds to the N-site of HIV-1 RT (Fig. 8C). Concentrations of approximately 300 nM are required to trap 50% of the complex population in the posttranslocational state. In contrast, the presence of an NNRTI (nevirapine) does not stabilize the posttranslocational state but causes a loss of cleavage at position −18. This probably reflects the conformational change upon inhibitor binding. It has earlier been reported that NNRTI binding affects the position of RNase H cleavage (22).

INDOPY-1 has a unique resistance profile. The different chemical structure and mechanism of action of INDOPY-1, compared to those of NRTIs and NNRTIs, suggests that the resistance profile of this novel compound class may differ from currently used HIV RT inhibitors. To address this question, we assessed the phenotypic susceptibility of over 6,000 clinical HIV-1 isolates for INDOPY-1 and different NRTIs and NNRTIs. Over 80% of the profiled clinical isolates remain susceptible to INDOPY-1, which was defined as having a less-than-fourfold increase in EC_{50} compared to wild-type susceptibility. No cross-resistance was observed between INDOPY-1 and the NNRTI efavirenz or nevirapine or the NRTI didanosine, stavudine, tenofovir, zalcitabine, or zidovudine (Pearson correlation coefficient [r] < 0.2). However, phenotypic cross-resistance was detected with NRTIs abacavir (r = 0.32) and lamivudine (r = 0.56).

Genotypic analyses of more than 1,700 of these clinical isolates showed that the combination of mutations M184V and Y115F is associated with reduced susceptibility and that the presence of K65R confers increased susceptibility to INDOPY-1 (Table 3). In contrast, thymidine analogue-associated mutations (TAMs) (11, 14, 18) show no association with a change in INDOPY-1 susceptibility.

Site-directed mutant strains further confirmed that INDOPY-1 activity is not affected by the presence of TAMs or any of the other major NRTI-induced, multidrug-resistant mutations: the T69 insertion complex (17) and the Q151M complex (13) (Table 4). Site-directed mutant strains with single mutations M184V and Y115F showed moderate changes (5.0- and 7.9-fold changes, respectively), whereas the combination of both mutations resulted in a large change (>100-fold change). Moreover, we found that the combination of mutations M184V and Y115F emerges under the selective pressure of INDOPY-1 (data not shown). As mutation M184V is known to cause high-level resistance (>100-fold change) to lamivudine and intermediate resistance to abacavir (21), the presence of this mutation explains the limited cross-resistance seen with INDOPY-1. Using SDM strains, we also verified the influence of the K65R mutation on INDOPY-1 susceptibility, as seen in clinical isolates. In contrast with lamivudine or abacavir where the presence of K65R is associated with a reduced susceptibility (21), the mutation causes an increase in susceptibility for INDOPY-1. Likewise, the presence of K65R in a background of the M184V mutation restores sensitivity to INDOPY-1. Amino acids Lys^{65}, Met^{184}, and Tyr^{115} are all located at or in close proximity to the active center of HIV-1 RT ahead of the 3′ end of the primer (12). This provides genetic evidence for the notion that INDOPY-1 binds to the nucleotide binding site.

To further verify the binding properties of the inhibitor, we studied whether the two major mutations conferring resistance, M184V and Y115F, can affect the ability of INDOPY-1 to compete with the nucleotide substrate. For this purpose, we

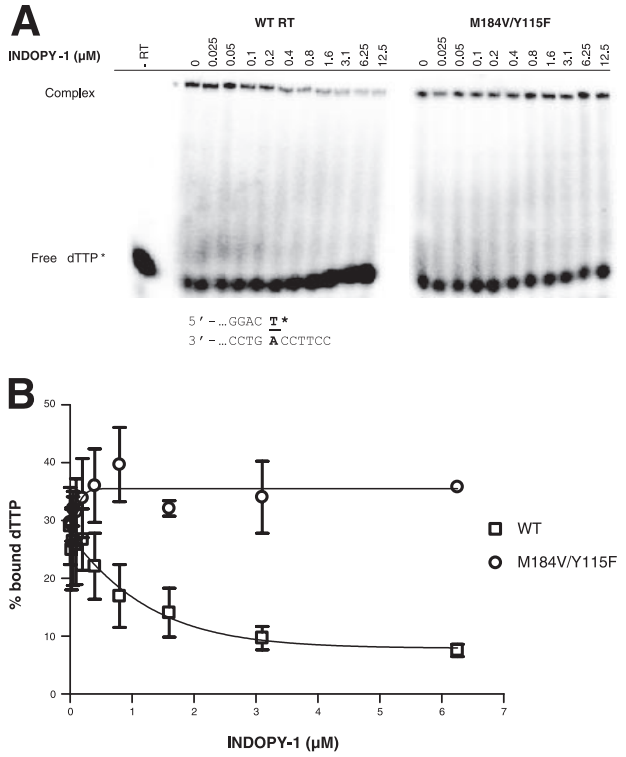

FIG. 9. Competition between INDOPY-1 and the nucleotide substrate. (A) Wild-type (WT) RT and the M184V Y115F double mutant were incubated with a DNA/DNA substrate and a radiolabeled nucleotide (dTTP). The DNA primer contained a dideoxycytidine at its 3′ end to prevent incorporation of the nucleotide. The complex was challenged with increasing concentrations of INDOPY-1, and the samples were analyzed on nondenaturing gels. The relevant sequences are shown below the band shift experiment. (B) Graphic representation of the data shown in panel A. The values shown are averages ± standard deviations (error bars) from three independent experiments.

performed band shift experiments with a radiolabeled nucleotide (Fig. 9). Both wild-type RT and a mutant enzyme containing the M184V and Y115F mutations, form a stable ternary complex with the DNA/DNA primer/template and bound dNTP. The stability of the complex with the wild-type enzyme is compromised in the presence of increasing concentrations of INDOPY-1. In contrast, the stability of the ternary complex with the mutant enzyme is not affected under the same conditions. These findings suggest that the two mutations reduce binding of INDOPY-1 and, in turn, its ability to compete with a natural nucleotide substrate.

Conclusion. Taken together, different, complementary sets of biochemical and cellular experiments presented in this study show that compounds other than nucleotide or pyrophosphate analogues can bind the active center of HIV-1 RT, thus inhibiting enzymatic activity. NRTIs and INDOPY-1 show fundamentally different requirements with respect to the involvement of primer/template sequences in inhibitor binding. Binding of INDOPY-1 is not based on Watson and Crick base pairing with the template, it depends on structural features at, and in close proximity to, the 3′ end of the primer. Its mode of action includes competition with the incoming nucleotides for binding at the active site of RT. This novel mechanism of action translates in a unique resistance profile. While the presence of mutations M184V and Y115F in RT is associated with a decreased susceptibility, the presence of K65R is associated with an increased susceptibility for INDOPY-1.

ACKNOWLEDGMENTS

We thank R. Pauwels for guidance through the early phase of these studies. Susceptibility measurements on clinical HIV-1 isolates were done in collaboration with Virco BVBA. We thank Anik Peeters for creative discussions and Luc Geeraert for excellent editorial help.

J.D. is the recipient of a postdoctoral fellowship from the Canadian Institutes of Health Research (CIHR). HIV research in M.G.'s laboratory is sponsored by the CIHR, and this study was cosponsored by Tibotec. M.G. is the recipient of a national career award (CIHR).

REFERENCES

1. **Arts, E. J., X. Li, Z. Gu, L. Kleiman, M. A. Parniak, and M. A. Wainberg.** 1994. Comparison of deoxyoligonucleotide and tRNA(Lys-3) as primers in an endogenous human immunodeficiency virus-1 in vitro reverse transcription/template-switching reaction. J. Biol. Chem. **269:**14672–14680.
2. **Balzarini, J., R. Pauwels, M. Baba, M. J. Robins, R. M. Zou, P. Herdewijn, and E. De Clercq.** 1987. The 2′,3′-dideoxyriboside of 2,6-diaminopurine selectively inhibits human immunodeficiency virus (HIV) replication in vitro. Biochem. Biophys. Res. Commun. **145:**269–276.
3. **Balzarini, J., M.-J. Perez-Perez, A. San-Felix, M.-J. Camarasa, I. C. Bathurst, P. J. Barr, and E. De Clercq.** 1992. Kinetics of inhibition of human immunodeficiency virus type 1 (HIV-1) reverse transcriptase by the novel HIV-1-specific nucleoside analogue [2′,5′-bis-O-(tert-butyldimethylsilyl)-beta-D-ribofuranosyl]-3′-spiro-5″-(4″-amino-1″,2″-oxathiole-2″, 2″-dioxide)thymine (TSAO-T). J. Biol. Chem. **267:**11831–11838.
4. **Clavel, F., and A. J. Hance.** 2004. HIV drug resistance. N. Engl. J. Med. **350:**1023–1035.
5. **De Clercq, E.** 2003. Clinical potential of the acyclic nucleoside phosphonates cidofovir, adefovir, and tenofovir in treatment of DNA virus and retrovirus infections. Clin. Microbiol. Rev. **16:**569–596.
6. **Delwart, E. L., E. G. Shpaer, J. Louwagie, F. E. McCutchan, M. Grez, H. Rubsamen-Waigmann, and J. I. Mullins.** 1993. Genetic relationships determined by a DNA heteroduplex mobility assay: analysis of HIV-1 env genes. Science **262:**1257–1261.
7. **Division of AIDS, National Institute of Allergy and Infectious Diseases, National Institutes of Health, and Collaborating Investigators.** 1997. Virology manual for HIV laboratories. Publication NIH-97-3828. U.S. Department of Health and Human Services, Washington, D.C.
8. **Furman, P. A., J. A. Fyfe, M. H. St. Clair, K. Weinhold, J. L. Rideout, G. A. Freeman, S. N. Lehrman, D. P. Bolognesi, S. Broder, H. Mitsuya, and D. W. Barry.** 1986. Phosphorylation of 3′-azido-3′-deoxythymidine and selective interaction of the 5′-triphosphate with human immunodeficiency virus reverse transcriptase. Proc. Natl. Acad. Sci. USA **83:**8333–8337.
9. **Goody, W. S., B. Müller, and T. Westle.** 1991. Factors contributing to the inhibition of HIV reverse transcriptase by chain-terminating nucleotides in vitro and in vivo. FEBS Lett. **291:**1–5.
10. **Hertogs, K., M.-P. de Béthune, V. Miller, T. Ivens, P. Schel, A. Van Cauwenberge, C. Van den Eynde, V. van Gerwen, H. Azijn, M. van Houtte, F. Peeters, S. Staszewski, M. Conant, S. Bloor, S. Kemp, B. Larder, and R. Pauwels.** 1998. A rapid method for simultaneous detection of phenotypic resistance to inhibitors of protease and reverse transcriptase in recombinant human immunodeficiency virus type 1 isolates from patients treated with antiretroviral drugs. Antimicrob. Agents Chemother. **42:**269–276.
11. **Hooker, D. J., G. Tachedjian, A. E. Solomon, A. D. Gurusinghe, S. Land, C. Birch, J. L. Anderson, B. M. Roy, E. Arnold, and N. J. Deacon.** 1996. An in vivo mutation from leucine to tryptophan at position 210 in human immunodeficiency virus type 1 reverse transcriptase contributes to high-level resistance to 3′-azido-3′-deoxythymidine. J. Virol. **70:**8010–8018.
12. **Huang, H., R. Chopra, G. L. Verdine, and S. C. Harrison.** 1998. Structure of a covalently trapped catalytic complex of HIV-1 reverse transcriptase: implications for drug resistance. Science **282:**1669–1675.
13. **Iversen, A. K. N., R. W. Shafer, K. Wehrly, M. A. Winters, J. I. Mullins, B. Chesebro, and T. C. Merigan.** 1996. Multidrug-resistant human immunodeficiency virus type 1 strains resulting from combination antiretroviral therapy. J. Virol. **70:**1086–1090.
14. **Kellam, P., C. A. Boucher, and B. A. Larder.** 1992. Fifth mutation in human immunodeficiency virus type 1 reverse transcriptase contributes to the development of high-level resistance to zidovudine. Proc. Natl. Acad. Sci. USA **89:**1934–1938.
15. **Kesteleyn, B., W. Van De Vreken, N. Kindermans, M. Canard, K. Hertogs, E. Bettens, V. De Vroey, D. Jochmans, P. Wigerinck, A. Tahri, J. Wang, and D. Surleraux.** 2004. Substituted indolepyridinium as anti-infective compounds. Patent WO2004046143.

16. **Kopp, E. B., J. J. Miglietta, A. G. Shrutkowski, C.-K. Shih, P. M. Grob, and M. T. Skoog.** 1991. Steady state kinetics and inhibition of HIV-1 reverse transcriptase by a non-nucleoside dipyridodiazepinone, BI-RG-587, using a heteropolymeric template. Nucleic Acids Res. **19:**3035–3039.
17. **Larder, B., S. Bloor, S. D. Kemp, K. Hertogs, R. Desmet, V. Miller, M. Sturmer, S. Staszewski, J. Ren, D. K. Stammers, D. I. Stuart, and R. Pauwels.** 1999. A family of insertion mutations between codons 67 and 70 of human immunodeficiency virus type 1 reverse transcriptase confer multinucleoside analog resistance. Antimicrob. Agents Chemother. **43:**1961–1967.
18. **Larder, B. A., and S. D. Kemp.** 1989. Multiple mutations in HIV-1 reverse transcriptase confer high-level resistance to zidovudine (AZT). Science **246:**1155–1158.
19. **Larder, B. A., A. Kohli, P. Kellam, S. D. Kemp, M. Kronick, and R. D. Henfrey.** 1993. Quantitative detection of HIV-1 drug resistance mutations by automated DNA sequencing. Nature **365:**671–673.
20. **Marchand, B., and M. Götte.** 2003. Site-specific footprinting reveals differences in the translocation status of HIV-1 reverse transcriptase. Implications for polymerase translocation and drug resistance. J. Biol. Chem. **278:**35362–35372.
21. **Miller, V., and B. A. Larder.** 2001. Mutational patterns in the HIV genome and cross-resistance following nucleoside and nucleotide analogue drug exposure. Antivir. Ther. **6:**25–44.
22. **Palaniappan, C., P. J. Fay, and R. A. Bambara.** 1995. Nevirapine alters the cleavage specificity of ribonuclease H of human immunodeficiency virus 1 reverse transcriptase. J. Biol. Chem. **270:**4861–4869.
23. **Pauwels, R., K. Andries, J. Desmyter, D. Schols, M. J. Kukla, H. J. Breslin, A. Raeymaeckers, J. Van Gelder, R. Woestenborghs, J. Heykants, K. Schellekens, M. A. C. Janssen, E. De Clercq, and P. A. J. Janssen.** 1990. Potent and selective inhibition of HIV-1 replication in vitro by a novel series of TIBO derivatives. Nature **343:**470–474.
24. **Pauwels, R., J. Balzarini, M. Baba, R. Snoeck, D. Schols, P. Herdewijn, J. Desmyter, and E. De Clercq.** 1988. Rapid and automated tetrazolium-based colorimetric assay for the detection of anti-HIV compounds. J. Virol. Methods **20:**309–321.
25. **Rittinger, K., G. Divita, and R. S. Goody.** 1995. Human immunodeficiency virus reverse transcriptase substrate-induced conformational changes and the mechanism of inhibition by nonnucleoside inhibitors. Proc. Natl. Acad. Sci. USA **92:**8046–8049.
26. **Ryabova, S. Y., L. M. Alekseeva, and B. G. Granik.** 2000. 1H-pyrido[3,2-b]indoles: synthesis and investigation of some of their spectroscopic and chemical properties. Chem. Heterocyclic Compounds **36:**301–306.
27. **Ryabova, S. Y., N. Z. Tugusheva, L. M. Alekseeva, and V. G. Granik.** 1996. 3-Arylaminoindoles in the synthesis of indolo[3,2-b]quinoline derivatives. Pharm. Chem. J. **30:**472–477.
28. **Sarafianos, S. G., A. D. J. Clark, K. Das, S. Tuske, J. J. Birktoft, P. Ilankumaran, A. R. Ramesha, J. M. Sayer, D. M. Jerina, P. L. Boyer, S. H. Hughes, and E. Arnold.** 2002. Structures of HIV-1 reverse transcriptase with pre- and post-translocation AZTMP-terminated DNA. EMBO J. **21:**6614–6624.
29. **Smerdon, S. J., J. Jager, J. Wang, L. A. Kohlstaedt, A. J. Chirino, J. M. Friedman, P. A. Rice, and T. A. Steitz.** 1994. Structure of the binding site for nonnucleoside inhibitors of the reverse transcriptase of human immunodeficiency virus type 1. Proc. Natl. Acad. Sci. USA **91:**3911–3915.
30. **Spence, R. A., W. M. Kati, K. S. Anderson, and K. A. Johnson.** 1995. Mechanism of inhibition of HIV-1 reverse transcriptase by nonnucleoside inhibitors. Science **267:**988–993.
31. **St. Clair, M. H., C. Richards, T. Spector, K. Weinhold, W. Miller, A. Langlois, and P. A. Furman.** 1987. 3′-Azido-3′-deoxythymidine triphosphate as an inhibitor and substrate of purified human immunodeficiency virus reverse transcriptase. Antimicrob. Agents Chemother. **31:**1972–1977.
32. **Sterne, J. A. C., M. A. Hernán, B. Ledergerber, K. Tilling, R. Weber, P. Sendi, M. Rickenbach, J. M. Robins, M. Egger, and the Swiss HIV Cohort Study.** 2005. Long-term effectiveness of potent antiretroviral therapy in preventing AIDS and death: a prospective cohort study. Lancet **366:**378–384.
33. **Tong, W., C.-D. Lu, S. K. Sharma, S. E. Matsuura, A. G. So, and W. A. Scott.** 1997. Nucleotide-induced stable complex formation by HIV-1 reverse transcriptase. Biochemistry **36:**5749–5757.
34. **Witvrouw, M., C. Pannecouque, K. Van Laethem, J. Desmyter, E. De Clercq, and A.-M. Vandamme.** 1999. Activity of non-nucleoside reverse transcriptase inhibitors against HIV-2 and SIV. AIDS **13:**1477–1483.